Impact of oxygen on the permanent deactivation of boron–oxygen-related recombination centers in crystalline silicon

Bianca Lim,[a] Karsten Bothe, and Jan Schmidt
Institut für Solarenergieforschung Hameln (ISFH), Am Ohrberg 1, D-31860 Emmerthal, Germany

(Received 15 March 2010; accepted 24 April 2010; published online 18 June 2010)

The carrier lifetime in boron-doped Czochralski-grown silicon is ultimately limited by light-induced boron–oxygen-related recombination centers. These centers can be permanently deactivated by illumination at elevated temperature (70–220 °C). However, the detailed defect reactions leading to permanent deactivation are still unresolved. In this work, we study the impact of oxygen on the deactivation process. We examine the dependence of the deactivation rate on the interstitial oxygen concentration as well as the impact of long-term annealing at 450 °C, leading to the generation of oxygen clusters acting as donors (thermal donors). We find a decrease in the deactivation rate with both increasing interstitial oxygen concentration and increasing thermal donor concentration, suggesting that oxygen is involved in the deactivation process. © *2010 American Institute of Physics*. [doi:10.1063/1.3431359]

I. INTRODUCTION

The carrier lifetime in boron-doped oxygen-rich silicon is ultimately limited by light-induced boron–oxygen-related recombination centers, limiting the efficiency of solar cells fabricated on this material.[1] A permanent deactivation of these centers can be achieved by illumination at temperatures in the range of 70–220 °C.[2–5] This permanent deactivation effect has been observed in lifetime samples[4] as well as in solar cells.[3,5,6] However, seemingly inconsistent results regarding the rate at which the deactivation proceeds have been published,[3,4,6,7] suggesting a dependence of the involved defect reactions on a number of hitherto unresolved parameters. Recently, we have shown that the deactivation rate depends inversely on the total boron concentration, suggesting that boron is directly involved in the deactivation process.[8] In this work, we study the impact of oxygen on the deactivation process and surprisingly find a reciprocal dependence of the deactivation rate R_{de} on the interstitial oxygen concentration $[O_i]$. In addition, we observe that the formation of thermal donors (TDs), which are known to be oxygen clusters generated during long-term annealing at 450 °C, can slow down the deactivation process by more than a factor of 3. These results suggest that oxygen in some form is involved in the permanent deactivation process.

II. EXPERIMENTAL DETAILS

We use 0.72 Ω cm boron-doped Czochralski-grown silicon (Cz-Si) wafers with interstitial oxygen concentrations $[O_i]$ in the range of $[O_i]=(2.5–5.1)\times10^{17}$ cm^{-3}, as determined according to DIN 50438–1 using a Bruker Equinox 55 Fourier transform infrared spectrometer. The samples underwent a thermal donor annihilation step (i.e., annealing at 750 °C for 30 min in N_2) and were RCA cleaned before being passivated by either plasma-enhanced chemical-vapor deposited (PECVD) silicon nitride (SiN_x) (Ref. 9) or plasma-assisted atomic layer deposited (PA-ALD) aluminum oxide (Al_2O_3).[10] The substrate temperature during atomic layer deposition was set at 200 °C, the layer thickness was 30 nm and following deposition the samples were annealed for 15 min at 425 °C.

These two different forms of passivation were chosen with regard to recent reports on the impact of hydrogen-rich SiN_x films on the deactivation process.[7] The standard passivation technique used in carrier lifetime studies today is the deposition of hydrogen-rich [~16–18 at. % H (Refs. 11 and 12)] PECVD silicon nitride. Regarding the surface passivation of *p*-type silicon samples, however, ALD-Al_2O_3 has recently been found to be extremely effective.[10,13,14] Since these Al_2O_3 films contain very little hydrogen (~3 at. % H),[15] it is important to investigate if permanent deactivation of boron–oxygen centers is possible in samples passivated with hydrogen-lean ALD-Al_2O_3, too.

The material used to examine the role of thermal donors is 0.8 Ω cm B-doped Cz-Si with an interstitial oxygen concentration of $[O_i]=(7–8)\times10^{17}$ cm^{-3}. All samples underwent acidic damage etching and thermal donor annihilation, followed by RCA-cleaning and PECVD-SiN_x coating. The SiN_x coating was used as a diffusion barrier to prevent metal contamination during the long-term anneals at 450 °C. Note that we coated all samples, even those that were not annealed at 450 °C, to ensure an as similar processing sequence as possible for all samples. The samples were then split into four groups: the control samples and three groups that were annealed at 450 °C in air for 8 h, 16 h, and 32 h, respectively. Subsequently, the silicon nitride was removed from all samples by a short etch in HF, the samples were RCA-cleaned and passivated by PA-ALD-Al_2O_3. The atomic layer deposition was again followed by a 15 min anneal at 425 °C. The thermal donor concentration was determined by measuring the resistivity of the samples before and after annealing. The treatment at 450 °C resulted in thermal donor concentrations of $[TD]_{8h}=1.7\times10^{15}$ cm^{-3}, $[TD]_{16h}=2.2$

[a]Author to whom correspondence should be addressed. Electronic mail: lim@isfh.de.

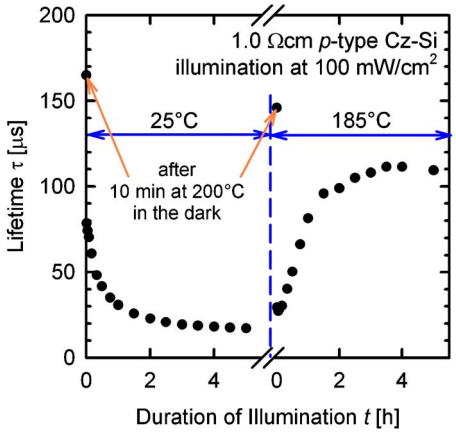

FIG. 1. (Color online) Typical evolution of the carrier lifetime τ under illumination in a 1.0 Ω cm B-doped Cz-Si sample passivated with PECVD-SiN_x. At room temperature (25 °C), the carrier lifetime decreases (left of dashed line). At 185 °C, τ increases until it saturates (right of dashed line). After this treatment, τ is stable under illumination at room temperature.

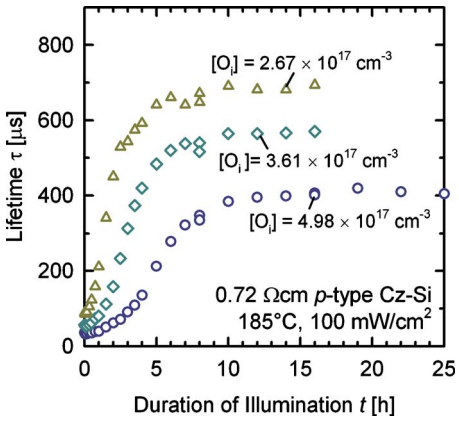

FIG. 2. (Color online) Lifetime τ of three 0.72 Ω cm B-doped Cz-Si samples passivated with Al_2O_3 plotted vs the duration of illumination t at 185 °C. The interstitial oxygen concentrations $[O_i]$ of the samples are 2.67×10^{17} cm^{-3} (triangles), 3.61×10^{17} cm^{-3} (diamonds), and 4.98×10^{17} cm^{-3} (circles). The saturation value of τ decreases with increasing $[O_i]$.

$\times10^{15}$ cm^{-3}, and $[TD]_{32h}=4.0\times10^{15}$ cm^{-3}, with a respective uncertainty of $[TD]_{err}=\pm0.3\times10^{15}$ cm^{-3}. No changes in resistivity exceeding this uncertainty were observed either after annealing the Al_2O_3 layers (15 min at 425 °C) or after the deactivation procedure (up to 40 h at 185 °C).

Lifetime measurements were performed at room temperature using the quasi-steady-state photoconductance technique.[16] The carrier lifetime τ was extracted at a fixed injection level of $\Delta n=1\times10^{15}$ cm^{-3} if not stated otherwise.

Illumination at elevated temperature was performed under a halogen lamp placed above a hotplate. The light intensity of 100 mW/cm^2 was adjusted using a calibrated solar cell. Over the course of one measurement (up to 50 h) the light intensity varied by up to 4%. The temperature of 185 °C was controlled by a proportional-integral-derivative controller with an uncertainty in the sample temperature of about ±5 °C.

III. RESULTS AND DISCUSSION

Figure 1 depicts the typical time dependence of the carrier lifetime τ in B-doped Cz-Si under illumination at room temperature (25 °C) and subsequently (beyond the dashed line in Fig. 1) at elevated temperature (185 °C). At $t=0$, all boron–oxygen-related centers are dissociated (after a 10 min anneal at 200 °C in the dark) and the lifetime is accordingly high ($\tau_0=165$ μs). At room temperature, the well-known light-induced degradation due to generation of boron–oxygen-related complexes can be observed,[1] after only 1 min, the lifetime drops to 78 μs, which is the so-called fast degradation. Subsequently, τ decreases at a slower rate, until reaching a saturation value (τ_d). Placing a sample under illumination at 185 °C (in the case shown after another 10 min anneal at 200 °C in the dark), we observe a very fast light-induced degradation, which is accelerated by the elevated temperature. However, subsequently the carrier lifetime recovers as the boron–oxygen complexes are deactivated. Subsequent illumination at room temperature has no further effect on the carrier lifetime.[4]

In Fig. 2, we plot the lifetime τ versus the duration of illumination t for three samples with different interstitial oxygen concentrations $[O_i]$. All samples have a resistivity of 0.72 Ω cm and were illuminated at 185 °C with a halogen lamp of 100 mW/cm^2 light intensity. As can be seen, the saturation value of the recovered lifetime decreases significantly with increasing interstitial oxygen concentration. The sample where $[O_i]=2.67\times10^{17}$ cm^{-3} recovers to a remarkably high lifetime of (690 ± 10) μs while the lifetime of the sample where $[O_i]=4.98\times10^{17}$ cm^{-3} saturates at (410 ± 10) μs.

Figure 3 shows the measured normalized defect concentration N_t^* (calculated from the lifetime data shown in Fig. 2) as a function of illumination time t. Here, N_t^* is defined as the difference of the inverse lifetime $\tau^{-1}(t)$ measured at time t and the inverse initial lifetime measured before degradation τ_0^{-1}, i.e., $N_t^*\equiv\tau^{-1}(t)-\tau_0^{-1}$. For better comparison, the maximum normalized defect concentration in each sample $N_{t\,max}^*$ is normalized to 1. On the double-logarithmic scale, the dif-

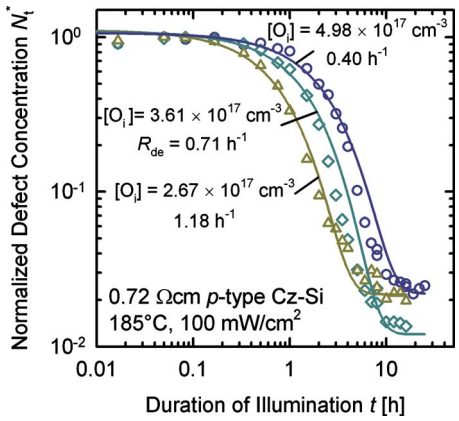

FIG. 3. (Color online) Normalized defect concentration N_t^* (calculated from the lifetime data shown in Fig. 2) of three 0.72 Ω cm B-doped Cz-Si samples with different interstitial oxygen concentrations $[O_i]$ plotted vs the duration of illumination t at 185 °C. The deactivation rate R_{de} is determined by an exponential fit to the data. As can be seen, R_{de} decreases with increasing $[O_i]$.

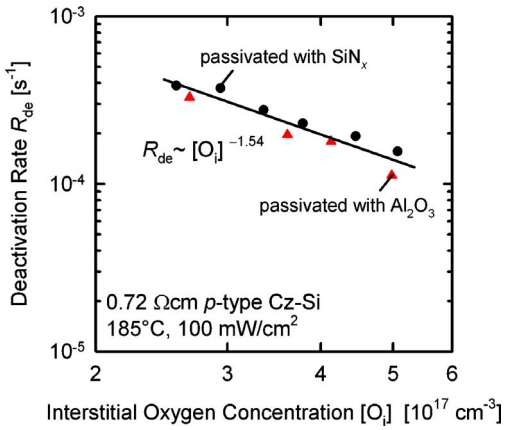

FIG. 4. (Color online) Measured deactivation rates R_{de} of 0.72 Ω cm B-doped Cz-Si samples at 185 °C and a light intensity of 100 mW/cm^2 plotted vs the interstitial oxygen concentration $[O_i]$. The circles correspond to samples passivated with hydrogen-rich SiN_x while the triangles correspond to samples passivated with hydrogen-lean Al_2O_3. There is no discernible difference between the two sets of samples. The overall dependence can be described by a power law $R_{de} \sim [O_i]^{-(1.54\pm0.20)}$.

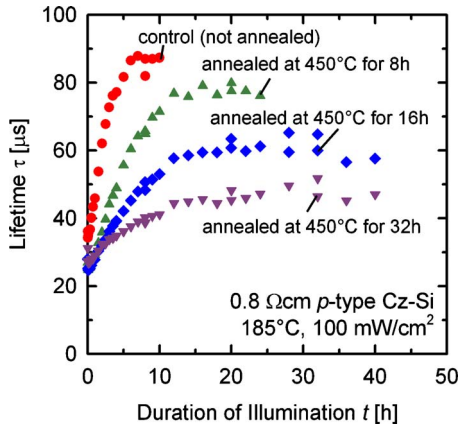

FIG. 5. (Color online) Time dependence of the carrier lifetime τ (measured at $\Delta n = 2\times10^{15}$ cm^{-3}) during illumination at 185 °C of four samples passivated with Al_2O_3. Three of the samples were annealed at 450 °C for 8 h, 16 h, and 32 h, respectively. The saturation lifetime decreases with increasing annealing time, the lifetime of the sample which was not annealed (circles) saturates at (87 ± 5) µs, while the final lifetime of the sample annealed for 32 h (triangles down) saturates at (45 ± 5) µs.

ference in the deactivation rates is easily distinguishable and it can be seen that the deactivation slows down with increasing interstitial oxygen concentration. Fitting the expression $N_t^*(t) = A\times\exp(-R_{de}t)+B$ to the experimental data gives the deactivation rate R_{de} for each sample.

The deactivation rates R_{de} for all investigated samples are plotted versus the interstitial oxygen concentrations $[O_i]$ in Fig. 4. As can be seen from Fig. 4, the deactivation procedure takes longer the higher the interstitial oxygen content is. The linear dependence displayed on the double-logarithmic scale reveals a power law with an exponent of $-(1.54\pm0.20)$, i.e., $R_{de}\sim[O_i]^{-(1.54\pm0.20)}$. Figure 4 includes samples passivated with PECVD-SiN_x (circles) as well as samples passivated with ALD-Al_2O_3 (triangles). Obviously, the permanent deactivation of the boron–oxygen-related centers proceeds in the same way for the Cz-Si wafers passivated with hydrogen-lean Al_2O_3, i.e., in the absence of a hydrogen-rich dielectric layer, as there is no discernable difference between the deactivation rates of the two groups of samples. There are two possible explanations for this observation: either hydrogen has no impact on the deactivation process at all, or the amount of hydrogen diffusing into the bulk of the wafers during the SiN_x deposition and the subsequent anneals is too small to have a discernible impact.

Thermal donor formation was performed during anneals at 450 °C in air for 8 h, 16 h, and 32 h, respectively. Figure 5 depicts the time dependence of the carrier lifetime τ (at an injection level of $\Delta n = 2\times10^{15}$ cm^{-3}) during illumination at 185 °C for all samples. The control wafer (circles), without any thermal donors, displays the fastest deactivation as well as the highest recovered lifetime of (87 ± 5) µs. With increasing thermal donor concentration, the deactivation slows down and the saturation value for the recovered lifetime decreases, leading to a final value of (77 ± 3) µs for the sample which had been annealed at 450 °C for 8 h (triangles up), (60 ± 5) µs for the sample annealed for 16 h (diamonds), and (45 ± 5) µs for the sample which was annealed for 32 h (triangles down).

Figure 6 shows the normalized defect concentration N_t^*, derived from the lifetimes shown in Fig. 5, as a function of the duration of illumination t on a double logarithmic scale. Note that the initial lifetimes measured before light-induced degradation τ_0 are not shown in Fig. 5 since they are above 100 µs. The control wafer without any thermal donors yields a deactivation rate of $R_{de}=0.64$ h^{-1}, which is more than three times the deactivation rate of the sample which was annealed at 450 °C for 32 h ($R_{de}=0.19$ h^{-1}). Figure 6 also shows that the final normalized defect concentration increases with increasing TD concentration. Apart from delaying the deactivation process, thermal donors thus also seem to reduce the efficacy of the deactivation process.

The deactivation rates R_{de} determined from Fig. 6 are plotted versus the thermal donor concentration in Fig. 7. The data can be fitted by a power law (line) of the form $R_{de}\sim[TD]^{-(0.38\pm0.16)}$.

We would like to point out that the decrease in R_{de} with increasing TD concentration is most likely not related to

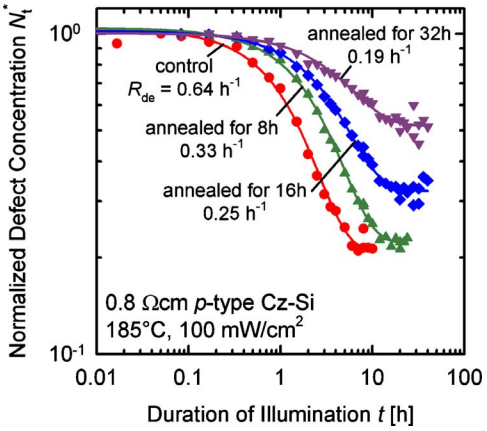

FIG. 6. (Color online) Normalized defect concentration N_t^* derived from the lifetime data in Fig. 5 plotted vs the duration of illumination t. The deactivation rate R_{de} decreases with increasing annealing times, from 0.64 h^{-1} (nonannealed control) to 0.19 h^{-1} (annealed for 32 h at 450 °C). In addition, the deactivation process is less effective after thermal donor formation.

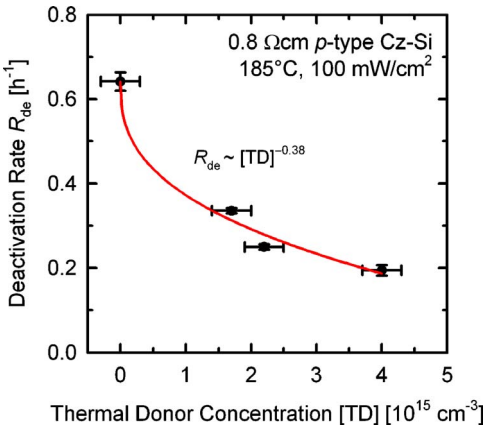

FIG. 7. (Color online) Dependence of the deactivation rate R_{de} on the thermal donor concentration [TD]. The decrease in R_{de} with increasing TD concentration can be described by a power law $R_{de} \sim [TD]^{-(0.38\pm0.16)}$.

compensation effects, i.e., the decrease in the equilibrium hole concentration p_0, since we very recently reported that the deactivation rate in compensated Cz-Si containing both boron and phosphorus scales inversely with the *total boron concentration* [B] (and not with the equilibrium hole concentration p_0).[8]

Since thermal donors are oxygen clusters, their impact on the deactivation rate and deactivation extent provides further evidence that oxygen-related defects are involved in the deactivation process.

IV. CONCLUSIONS

We have provided evidence that the permanent deactivation process of recombination-active boron–oxygen centers in B-doped Cz-Si proceeds in the same way in Cz-Si samples passivated with hydrogen-rich SiN_x and hydrogen-lean Al_2O_3. As a consequence, the presence of high amounts of hydrogen in the dielectric passivation layer alone does not influence the deactivation process. Our experiments of the permanent deactivation on Cz-Si wafers with various oxygen contents have revealed that the deactivation rate R_{de} depends inversely on the interstitial oxygen concentration $[O_i]$ following a power law of the form $R_{de} \sim [O_i]^{-(1.54\pm0.20)}$. In addition, the saturation value of the recovered lifetime decreases with increasing $[O_i]$. The presence of thermal donors was found to be detrimental to the deactivation process, both concerning the speed with which the deactivation proceeds and the extent to which the deactivation works. These findings strongly suggest that oxygen plays a decisive role in the physical mechanism behind the deactivation process.

[1] J. Schmidt and K. Bothe, Phys. Rev. B **69**, 024107 (2004).
[2] A. Herguth, G. Schubert, M. Kaes, and G. Hahn, *Proceedings of the 21st EUPVSEC*, Dresden, Germany (WIP, Munich, 2006), p.530.
[3] A. Herguth, G. Schubert, M. Kaes, and G. Hahn, Prog. Photovoltaics **16**, 135 (2008).
[4] B. Lim, K. Bothe, and J. Schmidt, phys. status solidi (RRL) **2**, 93 (2008).
[5] B. Lim, S. Hermann, K. Bothe, J. Schmidt, and R. Brendel, Appl. Phys. Lett. **93**, 162102 (2008).
[6] S. Dubois, N. Enjalbert, J. P. Garandet, R. Monna, and J. Kraiem, *Proceedings of the 23rd EUPVSEC*, Valencia, Spain (WIP, Munich, 2008), p.1437.
[7] K. A. Münzer, *Proceedings of the 24th EUPVSEC*, Hamburg, Germany (WIP, Munich, 2009), p.1558.
[8] B. Lim, A. Liu, D. Macdonald, K. Bothe, and J. Schmidt, Appl. Phys. Lett. **95**, 232109 (2009).
[9] T. Lauinger, J. Schmidt, A. G. Aberle, and R. Hezel, Appl. Phys. Lett. **68**, 1232 (1996).
[10] J. Schmidt, B. Veith, and R. Brendel, phys. status solidi (RRL) **3**, 287 (2009).
[11] B. Lenkeit, Ph.D. thesis, University of Hanover, 2002.
[12] T. Lauinger, Ph.D. thesis, University of Hanover, 2001.
[13] G. Agostinelli, A. Delabie, P. Vitanov, Z. Alexieva, H. F. W. Dekkers, S. De Wolf, and G. Beaucarne, Sol. Energy Mater. Sol. Cells **90**, 3438 (2006).
[14] B. Hoex, S. B. S. Heil, E. Langereis, M. C. M. van de Sanden, and W. M. M. Kessels, Appl. Phys. Lett. **89**, 042112 (2006).
[15] G. Dingemans, M. C. M. van de Sanden, and W. M. M. Kessels, Electrochem. Solid-State Lett. **13**, H76 (2010).
[16] R. Sinton and A. Cuevas, Appl. Phys. Lett. **69**, 2510 (1996).